Efficient Light Harvesting in a Dark, Hot, Acidic Environment

Thangaraj, Balakumar; Jolley, Craig C.; Sarrou, Iosifina; Bultema, Jelle B.; Greyslak, Jason; Whitelegge, Julian P.; Lin, Su; Kouril, Roman; Subramanyam, Rajagopal; Boekema, Egbert J.

Published in:
Biophysical Journal

DOI:
10.1016/j.bpj.2010.09.069

Publication date:
2011

Biophysical Journal

Supporting Material

Efficient light harvesting in a dark, hot, acidic environment: The structure and function of PSI-LHCI from *Galdieria sulphuraria*

Balakumar Thangaraj, Craig C. Jolley, Iosifina Sarrou, Jelle B. Bultema, Jason Greyslak, Julian P. Whitelegge, Su Lin, Roman Kouřil, Rajagopal Subramanyam, Egbert J. Boekema, and Petra Fromme

Fig. S1

P700 Extinction coefficient. The flash induced absorbance difference spectra of P700 and TMPD for *Galdieria* and *T.elongatus*. Each trace is an average of 3 different scans. The calculation of the extinction coefficient for P700 was based in the redox reaction of P700 with TMPD, in a method described previously (see materials and methods), using the formula below:

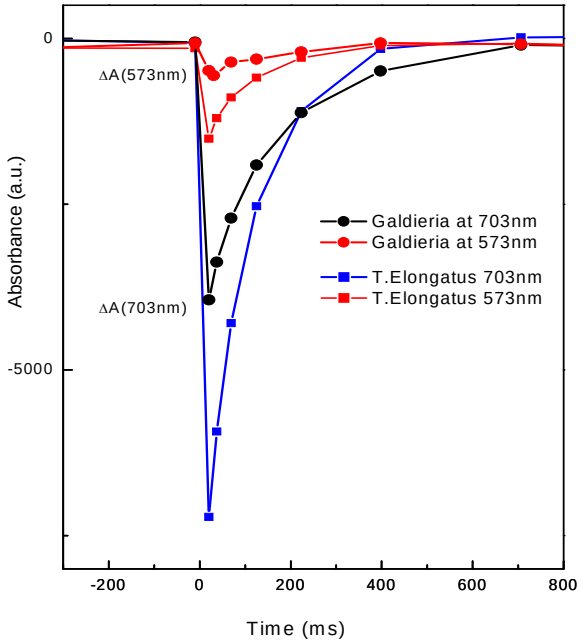

$$\Delta\varepsilon_{P700} = \Delta\varepsilon_{TMPD} \cdot \frac{\Delta A(703nm)}{\Delta A(573nm)}$$

Fig. S2

Oxidized minus reduced spectra of P700. Samples of *Galdieria* PSI-LHCI and *T.elongatus* PSI were suspended in 20 mM MES (pH 6.4), 100 mM $MgSO_4$ and 0.02 % β-DDM. Each trace is an average of three scans and the spectra were recorded at room temperature.

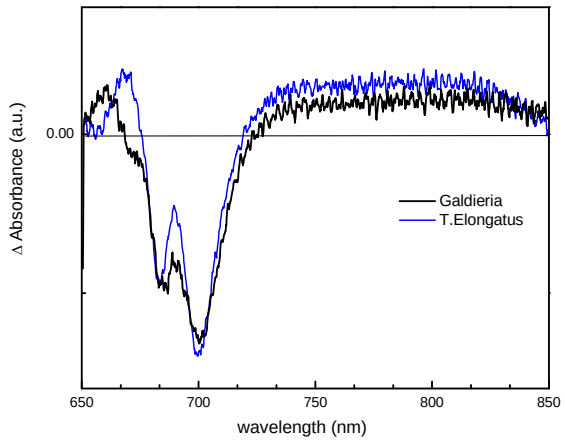

Fig. S3 and Table S1

MS/MS fragmentation of Lhcr1 peptide (**VPPVLAHDVYVK**) by Mascot software

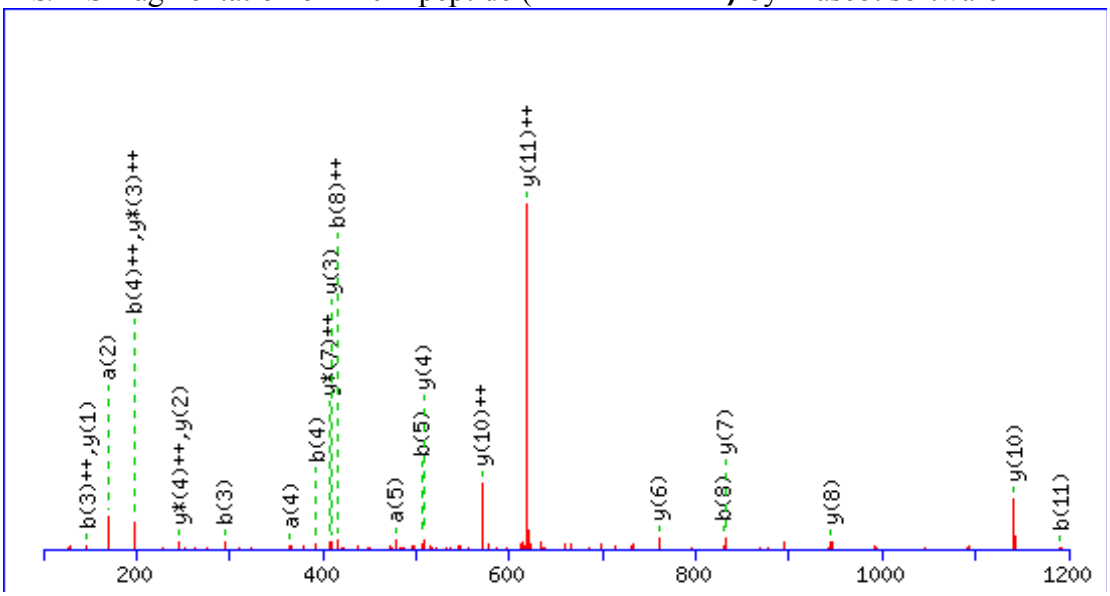

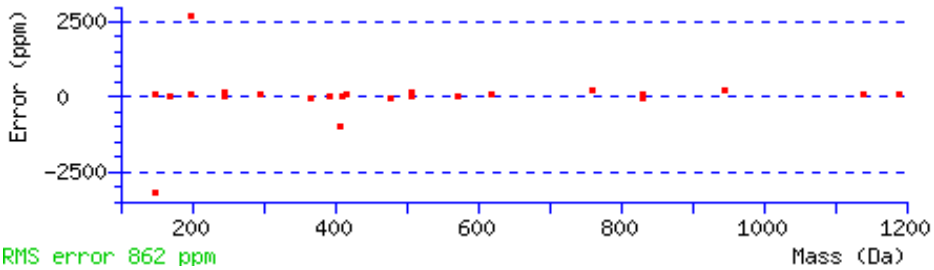

Monoisotopic mass of neutral peptide Mr(calc): 1335.7551
Ions Score: 56 Expect: 0.043
Matches (Bold Red): 25/88 fragment ions using 40 most intense peaks

#	a	a^{++}	b	b^{++}	Seq.	y	y^{++}	y^*	y^{*++}	#
1	72.0808	36.5440	100.0757	50.5415	V					12
2	**169.1335**	85.0704	**197.1285**	99.0679	P	1237.6939	**619.3506**	1220.6674	610.8373	11
3	266.1863	133.5968	**294.1812**	**147.5942**	P	**1140.6412**	**570.8242**	1123.6146	562.3109	10
4	**365.2547**	183.1310	**393.2496**	**197.1285**	V	1043.5884	522.2978	1026.5619	513.7846	9
5	**478.3388**	239.6730	**506.3337**	253.6705	L	**944.5200**	472.7636	927.4934	464.2504	8
6	549.3759	275.1916	577.3708	289.1890	A	**831.4359**	416.2216	814.4094	**407.7083**	7
7	686.4348	343.7210	714.4297	357.7185	H	**760.3988**	380.7030	743.3723	372.1898	6
8	801.4618	401.2345	**829.4567**	**415.2320**	D	623.3399	312.1736	606.3134	303.6603	5
9	900.5302	450.7687	928.5251	464.7662	V	**508.3130**	254.6601	491.2864	**246.1468**	4
10	1063.5935	532.3004	1091.5884	546.2978	Y	**409.2445**	205.1259	392.2180	**196.6126**	3
11	1162.6619	581.8346	**1190.6568**	595.8320	V	**246.1812**	123.5942	229.1547	115.0810	2
12					K	**147.1128**	74.0600	130.0863	65.5468	1

Fig. S4 and Table S2

MS/MS fragmentation of Lhcr2 peptide (**EPGYFGFDPLGLGK**) by Mascot software

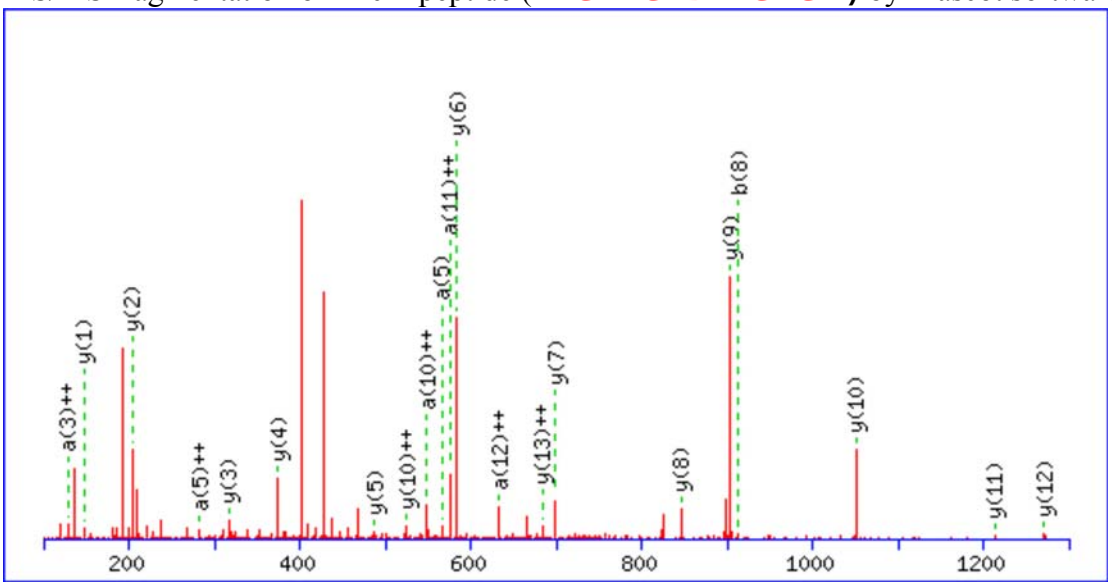

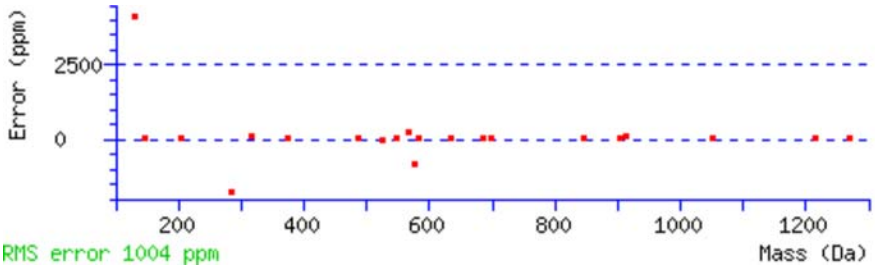

Monoisotopic mass of neutral peptide Mr(calc): 1495.7347
Fixed modifications: Carbamidomethyl (C)
Ions Score: 62 **Expect:** 0.01
Matches (Bold Red): 21/104 fragment ions using 68 most intense peaks

#	a	a^{++}	b	b^{++}	Seq.	y	y^{++}	y^*	y^{*++}	#
1	102.0550	51.5311	130.0499	65.5286	E					14
2	199.1077	100.0575	227.1026	114.0550	P	1367.6994	**684.3533**	1350.6729	675.8401	13
3	256.1292	**128.5682**	284.1241	142.5657	G	**1270.6467**	635.8270	1253.6201	627.3137	12
4	419.1925	210.0999	447.1874	224.0974	Y	**1213.6252**	607.3162	1196.5986	598.8030	11
5	**566.2609**	**283.6341**	594.2558	297.6316	F	**1050.5619**	**525.7846**	1033.5353	517.2713	10
6	623.2824	312.1448	651.2773	326.1423	G	**903.4934**	452.2504	886.4669	443.7371	9
7	770.3508	385.6790	798.3457	399.6765	F	**846.4720**	423.7396	829.4454	415.2264	8
8	885.3777	443.1925	**913.3727**	457.1900	D	**699.4036**	350.2054	682.3770	341.6921	7
9	982.4305	491.7189	1010.4254	505.7164	P	**584.3766**	292.6919	567.3501	284.1787	6
10	1095.5146	**548.2609**	1123.5095	562.2584	L	**487.3239**	244.1656	470.2973	235.6523	5
11	1152.5360	**576.7717**	1180.5310	590.7691	G	**374.2398**	187.6235	357.2132	179.1103	4
12	1265.6201	**633.3137**	1293.6150	647.3111	L	**317.2183**	159.1128	300.1918	150.5995	3
13	1322.6416	661.8244	1350.6365	675.8219	G	**204.1343**	102.5708	187.1077	94.0575	2
14					K	**147.1128**	74.0600	130.0863	65.5468	1

Fig. S5 and Table S3

MS/MS fragmentation of Lhcr3 peptide (**EPGYFGFDPLGLAK**) by Mascot software

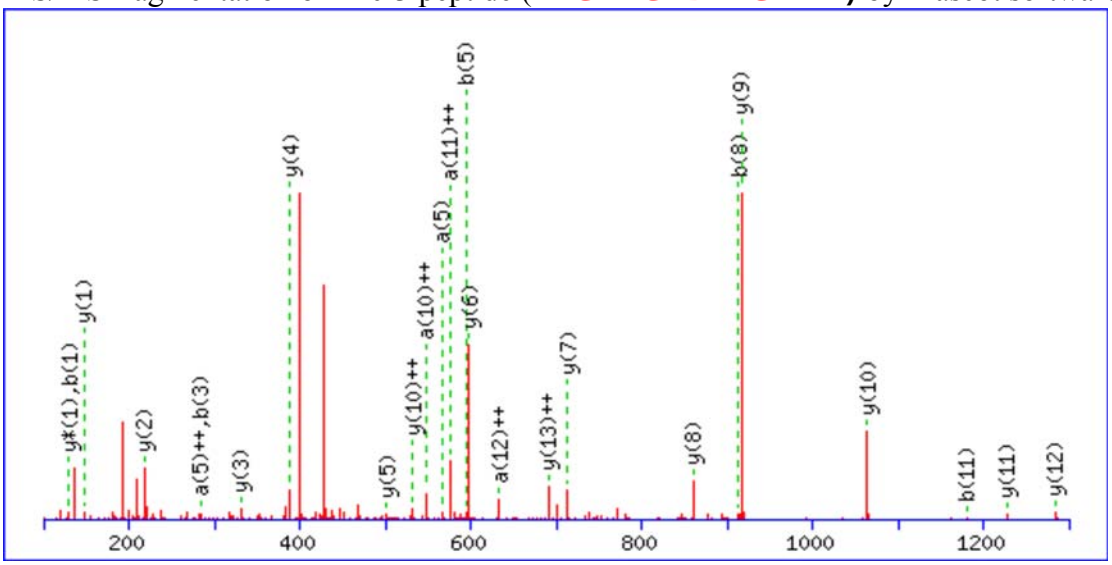

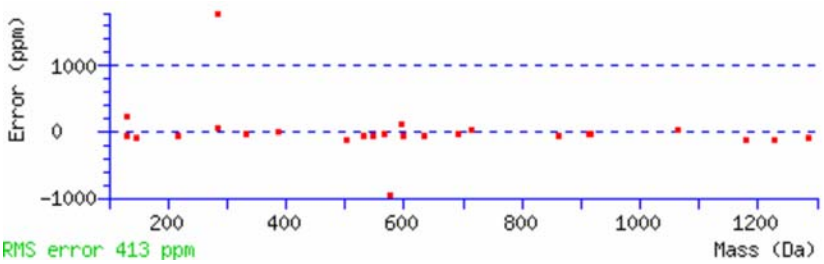

Monoisotopic mass of neutral peptide Mr(calc): 1509.7504
Fixed modifications: Carbamidomethyl (C)
Ions Score: 84 **Expect:** 6.2e-05
Matches (Bold Red): 25/104 fragment ions using 50 most intense peaks

#	a	a^{++}	b	b^{++}	Seq.	y	y^{++}	y^{*}	y^{*++}	#
1	102.0550	51.5311	**130.0499**	65.5286	E					14
2	199.1077	100.0575	227.1026	114.0550	P	1381.7151	**691.3612**	1364.6885	682.8479	13
3	256.1292	128.5682	**284.1241**	142.5657	G	**1284.6623**	642.8348	1267.6358	634.3215	12
4	419.1925	210.0999	447.1874	224.0974	Y	**1227.6408**	614.3241	1210.6143	605.8108	11
5	**566.2609**	**283.6341**	**594.2558**	297.6316	F	**1064.5775**	**532.7924**	1047.5510	524.2791	10
6	623.2824	312.1448	651.2773	326.1423	G	**917.5091**	459.2582	900.4825	450.7449	9
7	770.3508	385.6790	798.3457	399.6765	F	**860.4876**	430.7475	843.4611	422.2342	8
8	885.3777	443.1925	**913.3727**	457.1900	D	**713.4192**	357.2132	696.3927	348.7000	7
9	982.4305	491.7189	1010.4254	505.7164	P	**598.3923**	299.6998	581.3657	291.1865	6
10	1095.5146	**548.2609**	1123.5095	562.2584	L	**501.3395**	251.1734	484.3130	242.6601	5
11	1152.5360	**576.7717**	**1180.5310**	590.7691	G	**388.2554**	194.6314	371.2289	186.1181	4
12	1265.6201	**633.3137**	1293.6150	647.3111	L	**331.2340**	166.1206	314.2074	157.6074	3
13	1336.6572	668.8322	1364.6521	682.8297	A	**218.1499**	109.5786	201.1234	101.0653	2
14					K	**147.1128**	74.0600	**130.0863**	65.5468	1

Fig. S6 and Table S4

MS/MS fragmentation of Lhcr5 peptide (**LDESMPGYAGFDPLGFSDKFDVK**) by Mascot software

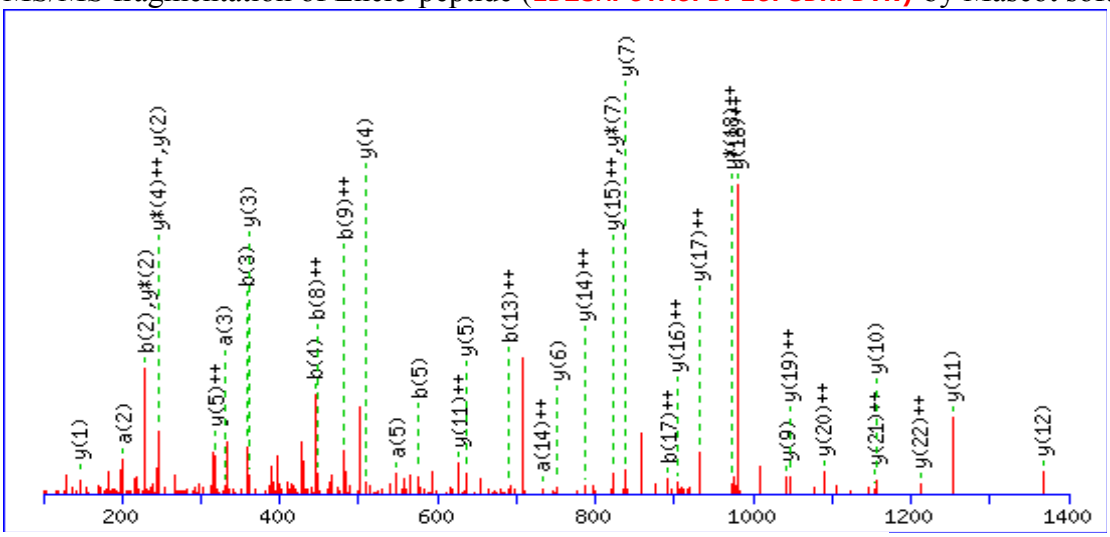

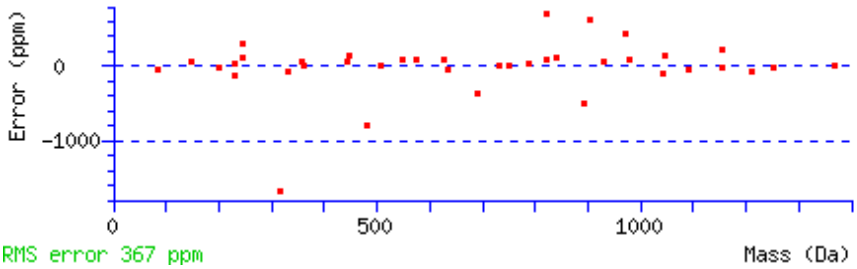

Monoisotopic mass of neutral peptide Mr(calc): 2534.1676
Ions Score: 71 **Expect:** 0.0012
Matches (Bold Red): 39/192 fragment ions using 98 most intense peaks

#	a	a++	a*	a*++	b	b++	b*	b*++	Seq.	y	y++	y*	y*++	#
1	86.0964	43.5519			114.0913	57.5493			L					23
2	201.1234	101.0653			229.1183	115.0628			D	2422.0908	1211.5490	2405.0642	1203.0357	22
3	330.1660	165.5866			358.1609	179.5841			E	2307.0638	1154.0355	2290.0373	1145.5223	21
4	417.1980	209.1026			445.1929	223.1001			S	2178.0212	1089.5142	2160.9947	1081.0010	20
5	548.2385	274.6229			576.2334	288.6203			M	2090.9892	1045.9982	2073.9626	1037.4850	19
6	645.2912	323.1493			673.2862	337.1467			P	1959.9487	980.4780	1942.9222	971.9647	18
7	702.3127	351.6600			730.3076	365.6574			G	1862.8959	931.9516	1845.8694	923.4383	17
8	865.3760	433.1917			893.3709	447.1891			Y	1805.8745	903.4409	1788.8479	894.9276	16
9	936.4131	468.7102			964.4081	482.7077			A	1642.8111	821.9092	1625.7846	813.3959	15
10	993.4346	497.2209			1021.4295	511.2184			G	1571.7740	786.3907	1554.7475	777.8774	14
11	1140.5030	570.7551			1168.4979	584.7526			F	1514.7526	757.8799	1497.7260	749.3666	13
12	1255.5300	628.2686			1283.5249	642.2661			D	1367.6842	684.3457	1350.6576	675.8324	12
13	1352.5827	676.7950			1380.5776	690.7925			P	1252.6572	626.8322	1235.6307	618.3190	11
14	1465.6668	733.3370			1493.6617	747.3345			L	1155.6045	578.3059	1138.5779	569.7926	10
15	1522.6883	761.8478			1550.6832	775.8452			G	1042.5204	521.7638	1025.4938	513.2506	9
16	1669.7567	835.3820			1697.7516	849.3794			F	985.4989	493.2531	968.4724	484.7398	8
17	1756.7887	878.8980			1784.7836	892.8954			S	838.4305	419.7189	821.4040	411.2056	7
18	1871.8156	936.4115			1899.8106	950.4089			D	751.3985	376.2029	734.3719	367.6896	6
19	1999.9106	1000.4589	1982.8841	991.9457	2027.9055	1014.4564	2010.8790	1005.9431	K	636.3715	318.6894	619.3450	310.1761	5
20	2146.9790	1073.9931	2129.9525	1065.4799	2174.9739	1087.9906	2157.9474	1079.4773	F	508.2766	254.6419	491.2500	246.1287	4
21	2262.0060	1131.5066	2244.9794	1122.9933	2290.0009	1145.5041	2272.9743	1136.9908	D	361.2082	181.1077	344.1816	172.5944	3
22	2361.0744	1181.0408	2344.0478	1172.5276	2389.0693	1195.0383	2372.0427	1186.5250	V	246.1812	123.5942	229.1547	115.0810	2
23									K	147.1128	74.0600	130.0863	65.5468	1

Fig. S7
Representative FDAS for *Galdieria* PSI-LHCI at 77K. The first three phases represent energy equilibration between the bulk and red-shifted antenna states and within the red-shifted population; the two slowest states represent fluorescence from thermally trapped red-shifted chlorophyll sites.

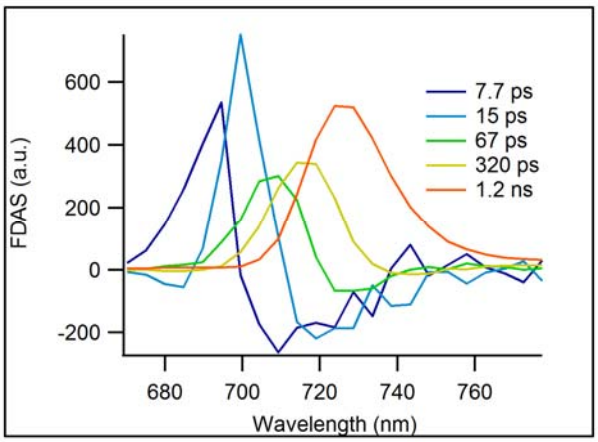

Fig. S8
Fluorescence decay-associated spectra obtained by time-correlated single photon counting (TCSPC) for *Galdieria* PSI-LHCI. The two dominant components arise from downhill energy transfer (7.6 ps) and trapping by P700 (70 ps).

Materials and methods:
Fluorescence decay kinetics were also measured using the time-correlated single-photon counting (TCSPC) technique. Excitation pulses of 130 fs at 400 nm, operated at 4 MHz were obtained from a Ti:S laser coupled to a frequency doubler and pulse selector (Spectra Physics, Millennia pumped Tsunami, and pulse selector Model 3980) Fluorescence emission was collected at 90° and detected using a double-grating monochromator (Jobin-Yvon, Gemini-180) and a microchannel plate photomultiplier tube (Hamamatsu R3809U-50). The polarization of the emission was 54.7° relative to that of the excitation. Data acquisition was done using a single photon counting card (Becker-Hickl, SPC-830). The IRF had a FWHM of 45 ps, measured from the scattering of sample at 400 nm. The excitation power was kept below 100 μW to avoid singlet-singlet annihilation. The data was fitted with a sum of exponential decay model globally or at a single wavelength using ASUFIT.

Results:
TCSPC recorded from 650 nm to 780 nm with a 10 nm interval. Four exponential components are necessary to fit the decay curves over the entire wavelength region (8 $\pm$ 1 ps, 60 $\pm$ 10 ps, 140 $\pm$ 10 ps, and 3.5 $\pm$ 1 ns). The first two decay components, showing lifetimes of 8 ps and 60 ps, dominate the entire wavelength region measured. Their spectral and temporal profiles are very similar to those obtained from streak camera measurements. The 8 ps component shows positive amplitude at the shorter wavelengths below 710 nm and negative amplitudes at the longer wavelengths, and the 60 ps component represents the overall decay of the fluorescence due to PSI core trapping. The two long-lived components peaking around 680 nm contribute only a few percent of the total fluorescence signal and probably originate from some loosely coupled (140 ps) and uncoupled (3.5 ns) antenna complexes. These two decay components likely originated from the same source as the 400-850 ps component in the room-temperature streak camera results but are better resolved in the TCSPC measurement because a higher signal-to-noise ratio can be achieved.